Journal of Environmental Science, Ecology & Chemistry

JESEC, 1(2), 88-95, 2025
https://doi.org/10.58985/jesec.2025.v01i02.09
eISSN: 0000-0000

Research Article

Sorption of Pb^{2+} and Cd^{2+} from Wastewater using Acid-Modified *Vigna Subterranea* Shell

Godwin Ogbaji Egah[1], Federick Teghtegh Samoh[2], Emmanuel Amuntse Yerima[1], Adelagun Ruth Olubukola Ajoke[1*] and Sarah Ateduobie Nwinee[3]

1. Department of Chemical Sciences, Federal University Wukari, Taraba State, Nigeria.
2. Department of Chemistry, University of Ilorin, Ilorin, Kwara State, Nigeria.
3. Science Laboratory Technology Department, Petroleum Training Institute, Effurun, Delta State, Nigeria.

Article Information
Received: 26 December 2024
Revised: 13 March 2025
Accepted: 18 March 2025
Published: 31 July 2025

Academic Editor
Prof. Dr. Giuseppe Oliveto

Corresponding Author
Prof. Dr. Adelagun Ruth Olubukola Ajoke
E-mail:
jemiruth2009@yahoo.com
Tel:

Keywords
Adsorption, wastewater, isotherm, kinetics, Vigna subterranea shell.

Abstract

The potential of acid-modified *Vigna subterranean* shells as an eco-friendly adsorbent for the removal of Pb^{2+} and Cd^{2+} ions from aqueous solutions was investigated in batch experiments. The effect of adsorbate pH was studied between pH 2-12 at 298 K. The adsorption thermodynamic was investigated at the range of 40°C - 80°C with 50 mL, of each adsorbate solution and the adsorbent dosage from 0.5 2.5 g at 1 h. An optimum adsorption efficiency of 99.784 (%) and 82.260 (%) was achieved for lead and cadmium at 298 K, respectively. Adsorption isotherms were studied by fitting the results obtained to different isotherm models, to elucidate the mechanism of interaction between the adsorbent and adsorbate. The results indicated that the Freundlich isotherm model adequately describes the interaction with R^2 values of 0.987 and 0.962 for lead and cadmium respectively, indicating a multilayer adsorption mechanism for lead and cadmium sorption by the adsorbent. R^2 values of 0.0800 and 0.0086 were obtained for the pseudo-first-order kinetic model plot, while 0.9999 and 0.9998 R^2 values were obtained for the pseudo-second-order model plot, an indicating that the adsorption process was best described by the Blanchard pseudo-second-order kinetic model, suggesting that chemisorption dominated the reaction. The positive values (+6.265 and +1.348 $kJmol^{-1}$) obtained for ΔH^0 for both lead and cadmium indicate an endothermic reaction.

1. Introduction

The global need for a pollution free environment seems to be failing, due to nonstop release of toxic heavy metals in the effluents from industrial discharges that are unfavorable to both flora and fauna. Heavy metals are highly toxic and persistent in the environment [1]. Heavy metals find applications in numerous industries including automobiles, batteries, pharmaceuticals, mining, electroplating, soap and detergents, textiles, paint, breweries and electroplating, however, their toxicity far exceeds the combined total toxicity of all radioactive and organic waste [2]. Heavy metals enter the body through food, air and water and bio-accumulate over time [3]. Several techniques have been reported for their removal from contaminated effluents, including chemical oxidation, coagulation–flocculation, membrane filtration, sedimentation, solvent extraction, ion exchange, reverse osmosis, evaporation, reduction and adsorption [4]. However, most of these methods, are expensive, inefficient,

inapplicable to a wide range of pollutants and generate toxic wastes that are difficult to treat [5]. The adsorption method has been widely reported for removing heavy metals because of its low-cost, flexibility and simplicity of design, ease of operation, availability and lack of harmful waste product formation [6, 7]. As a result, many scientists are seeking low-cost adsorbents, derived from agricultural waste, industrial by-products, natural materials, or modified biopolymers, algae, clay, zeolites, soil and sawdust [8, 9]. The increased volume of *Vigna subterranea* shells (VSS from Bambara nut) in the environment as agricultural waste has become an environmental concern due to pollution problems [10]. On the basis of green technology and turning waste to wealth, the potential of acidified *Vigna subterranea* shells (VSS) was investigated as adsorbents in the treatment of heavy metal contaminated wastewater.

2. Materials and methods

2.1. Adsorbent preparation and characterization

All the chemicals used were of high analytical grades. The VSS was collected from a local farm in Wukari LGA, Taraba State, Nigeria, washed and sun dried, grinded to powder and soaked in 0.1 M H_2SO_4 for 4 h [11]. Acid treatment was used to stabilize and retain the active sites of the VSS. The protonated VSH was then washed with deionized water, dried in an oven at 105 °C, crushed, sieved through a 150 - 250 mm mesh and stored as adsorbent. The surface functional groups of the adsorbent were investigated via Fourier Transform infrared spectroscopy in the range of 400 - 4000 cm^{-1} using the 5 % KBr disk method, while, a Sky-ray Instrument (EDX3600B X-ray fluorescence) was used to determine the chemical composition of the adsorbent.

2.2. Batch adsorption experiment

A batch experiment, as adopted by Egah *et al.*, [13] was carried out for the measurement of adsorption capacities. A 0.5 g of the adsorbent was contacted with 50 mL of varying initial concentrations (50-250 mg/L) of the adsorbate. It was then agitated at 300 rpm on a mechanical shaker for 1 h. Batch adsorption experiments were conducted to investigate the effects of pH, dosage, contact time, temperature and initial metal concentration. To investigate the effect of pH on the sorption process, 0.5 g of the adsorbent was added to 50 mL aliquots of 50 mg/L of the adsorbate at varying pH values (2-12) using 0.1 M HCl and 0.1 M NaOH. The effect of adsorbent dose on adsorption was studied using (0.5-2.5 g) adsorbent. The reaction mixture was allowed to equilibrate and filtered through a Whatman filter paper. The filtrates were analyzed using atomic adsorption spectrophotometer (Buck Scientific model 211 VGP) with the respective hollow cathode lamps to determine the residual concentrations of Pb^{2+} and Cd^{2+} at maximum wavelengths of 270 nm and 228.8 nm, respectively. The amount and percentage of adsorbate (lead and cadmium) adsorbed by the adsorbent was expressed as follows:

$$Q_{e\,(mg/g)} = \frac{(C_o - C_e)}{M_a} v \quad (1)$$

$$\text{Removal } (\%) = \left(\frac{C_o - C_e}{C_o}\right) \times 100 \quad (2)$$

where C_0 (mgL^{-1}) is the concentration of the adsorbate at the starting time (t = 0), Ce (mgL^{-1}) is the concentration of the adsorbate at equilibrium time, V (L) is the volume used in litre and M_a (g) is the mass of the adsorbent [15].

2.3. Adsorption isotherm

The Freundlich and Langmuir adsorption isotherms were used to describe the experimental data. The Freundlich isotherm model assumes that the removal of metal ions occurs on a heterogeneous adsorbent surface and can be related to multilayer adsorption [9]. The linear equation of the Freundlich isotherm is given as:

$$logQ_e = \frac{1}{n_f} logc_e + logK_f \quad (3)$$

Where Qe (mg/g) is the amount of adsorbate adsorbed per unit mass of adsorbent and Ce (mg/L) is the concentration at equilibrium. K_f is the Freundlich constants related to the adsorption capacity and nf the adsorption intensity [14]. A linear plot of logQe versus logCe gives n_F as the slope and K_f as the intercept. When the values of n are within the ranges of 1 - 10, they are referred to as good adsorption intensity [14]. The Langmuir adsorption isotherm is used for monolayer adsorption onto a surface containing a finite number of identical binding sites [13]. The Langmuir adsorption model is expressed as:

https://doi.org/10.58985/jesec.2025.v01i02.09

$$\frac{1}{Qe} = \frac{1}{Qm} + \frac{1}{Ce} \times \frac{1}{bQm} \quad (4)$$

Where Qm (mg/g) represents the total number of binding sites available for sorption, Ce is the equilibrium concentration of the adsorbate in bulk solution (mg/L), Qe (mg/g) is the amount of adsorbate adsorbed per unit mass of the adsorbent at equilibrium and b (L/mg) is the Adsorbate-Adsorbent Langmuir constant. A linear plot of $\frac{1}{Qe}$ versus $\frac{1}{Ce}$ gives a straight line graph, in which $\frac{1}{Qm}$ is the slope and $\frac{1}{bQm}$ is the intercept. The Langmuir isotherm characteristics are determined by the dimensionless constant known as the separation factor, R_L. This is expressed as:

$$R_L = \frac{1}{1+bC_o} \quad (5)$$

Where b (L/mg) is the Langmuir constant for adsorbate-adsorbent and C_o (mg/L) the initial adsorbate concentration. If $R_L > 1$, the adsorption is unfavourable, $R_L = 1$, adsorption is linear, R_L between 0-1, adsorption is favourable and $R_L = 0$, adsorption is irreversible [13, 16].

2.4. Adsorption kinetics studies

Chemical kinetics is used to determine how experimental conditions predict the rate of a chemical reaction. Pseudo-first-order and pseudo-second-order kinetic models were used to analyze the experimental data [9]. The Lagergren first-order equation is given by:

$$log(Q_e - Q_t) = logQ_e - \frac{K_1}{2.303}t \quad (6)$$

Where Qe is the amount of adsorbate sorbed per unit mass of the adsorbent (mg/g), Qt is the amount of adsorbate that was sorbed per unit time of the adsorbent (mg/g) at a contact time t (min) and k_1 is the pseudo first order rate constant ($Lmin^{-1}$). A plot of log (Qe - Qt) versus t gives k_1 which is the rate constant, while log Qe is the intercept and $-\frac{k_1}{2.303}$ the slope [17]. The equation is given by:

$$\frac{t}{Q_t} = \frac{1}{K_2 Q_{e^2}} + \frac{1}{Q_t}t \quad (7)$$

Where Q_t, Qe and t are as stated in first order model. K_2 ($g.mg^{-1}.min^{-1}$) is the pseudo-second rate constant and h (mg/g.min) = K_2Qe^2 is the initial adsorption rate.

A linear plot of $\frac{t}{Qt}$ versus t, gives K_2 as the second-order rate constant, $\frac{1}{k_2 Qe^2}$ as the intercept and $\frac{1}{Qe}$ as the slope [13].

2.5. Thermodynamics of adsorption

The thermodynamics parameters such as the enthalpy change ΔH^0 ($kJmol^{-1}$), entropy change ΔS^0 ($JK^{-1}mol^{-1}$) and free energy change ΔG^0 ($kJmol^{-1}$) were computed using the equation 8;

$$\text{Log}\left(\frac{q_e}{C_e}\right) = \frac{\Delta S^0}{2.303R} - \left(\frac{\Delta H^0}{2.303R}\right)\frac{1}{T} \quad (8)$$

Where ΔH^o and ΔS^o are change in enthalpy and changes in entropy respectively, log $\left(\frac{q_e}{C_e}\right)$ is the adsorption affinity, R is the represents universal gas constant (8.314 $Jmol^{-1}K^{-1}$) and T the temperature in (K). A plot of log $\left(\frac{q_e}{C_e}\right)$ versus $\frac{1}{T}$ gives a straight line graph where $\left(\frac{\Delta S^0}{2.303R}\right)$ is the intercept and-$\left(\frac{\Delta H^0}{2.303R}\right)$ is the slope [18, 19]. The Free Gibbs Energy is expressed as;

$$\Delta G° = \Delta H° - T\Delta S° \quad (9)$$

Where; T (k) represents the standard temperature taken to be 298 K.

3. Results and discussion

3.1. Characterization of the adsorbent

The results of the VSS FT-IR analysis in Fig. 1, reveal that the peaks at 3898.8 cm^{-1}, 3658 cm^{-1} and 3343.4 cm^{-1} are within the frequency range of (3000 - 4000 cm^{-1}) due to stretching vibrations of O-H groups capacity [13].

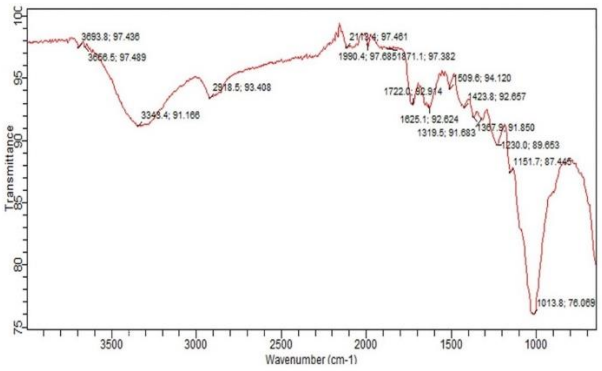

Figure 1. FTIR Spectrum of VSS.

The bands at 3898.8 cm^{-1} and 3658 cm^{-1} indicate the –OH groups at the edge of the VSS platelets capacity [20]. The bands at 3343.4 cm^{-1} are connected with the internal -OH stretching from hydroxyl groups

https://doi.org/10.58985/jesec.2025.v01i02.09

Table 1. FT-IR analysis of adsorbent.

Group Freq. (cm^{-1})	Functional groups	VSS	Assignment
	Alcohol/Phenol	3898.8	Free OH stretch
4000-3000	Alcohol/Phenol	3658	O-H stretch
	Alcohol/Phenol	3343.4	O-H stretch
3000 -2850	Alkanes	2918.5	C-H stretch
1730–1715	α, β –unsaturated esters	1722.0	C=O stretch
1650–1580	1° amines	1625.1	N–H bend
1500–1400	aromatics	1423.8	C–C stretch(in–ring)
1320–1000	carboxylic acid	1319.5	C–O stretch
1250–1020	Aliphatic amines	1230.0	C–N stretch

capacity [9]. The peak at 1625.1 cm^{-1} is attributed to N–H bending which is responsible for the binding of the adsorbent [13]. The peaks at 2918.5 cm^{-1}, 2113.4 cm^{-1}, and 1722.0 cm^{-1} are an indication of organic impurities in the VSS capacity [16]. Table 1 summarizes of the various peaks and functional groups assigned to each.

The chemical composition of the VSS adsorbent was determined using a Sky-ray Instrument (EDX3600B) X-Ray Florescence instrument (XRF), performed at a voltage of 40 kv and current of 350 µA. The XRF results showed that the chemical composition of the VSS sample was composed of: SO_3 (27.81 %) from sulphuric acid and K_2O (4.83 %) indicating a high grade adsorbent for the removal of lead and cadmium [13]. Others are P_2O_5 (0.861%), SiO_2 (2.37%), Al_2O_3 (2.03%), CaO (2.32%), Fe_2O_3 (0.43%), SnO_2 (2.15%) and Sb_2O_3 (2.15%) existing in small amount capacity [12].

3.2. Sorption experiments

3.2.1. *Effect of pH on sorption*

Fig. 2 shows the effect of pH on the adsorption of lead and cadmium by VSS. It was observed that optimum removal was achieved at pH 12 for lead and cadmium, which may be due to the increase in electrostatic attraction between the VSS adsorbent and the adsorbate [13]. However, as the pH approached an acidic pH at 2, there was an observed decrease in both lead and cadmium due to repulsion on the adsorbent surface, as the negative charges decreased [17]. The high adsorption at pH 12 showed that cation exchange was favored by alkaline pH [16].

3.2.2. Effect of adsorbent dosage on sorption

The effect of VSS dosage on the removal of lead and cadmium is shown in Fig. 3. The results showed that as the amount of the adsorbent was increased from 0.5

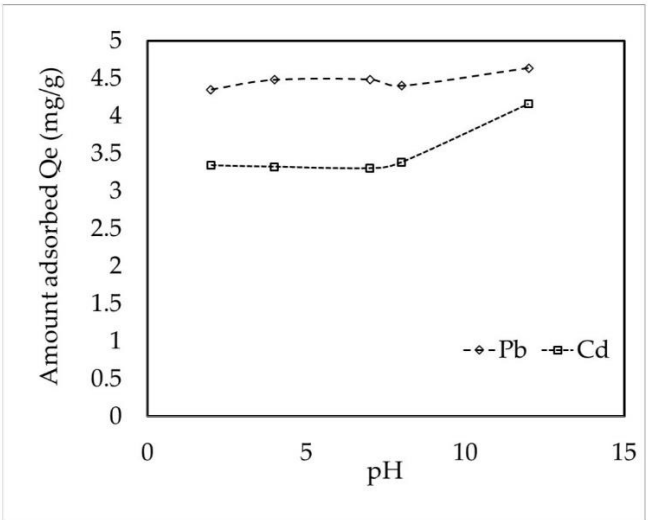

Figure 2. Effect of pH on sorption of Pb^{2+} and Cd^{2+} by VSS.

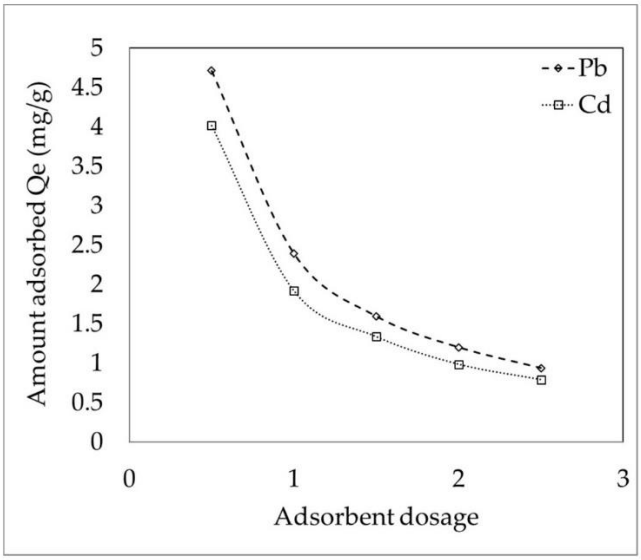

Figure 3. Effect of adsorbent dose on sorption of Pb^{2+} and Cd^{2+} by VSS.

https://doi.org/10.58985/jesec.2025.v01i02.09

to 2.5 g, the amount sorbed decreased from 0.940 to 4.715 mg/g and 0.792 to 4.016 mg/g for lead and cadmium, respectively. This is attributed to the large surface area available for adsorption, which enables adsorption to take place rapidly [13].

3.2.3. Effect of concentration on sorption

The results in Fig. 4 showed the effect of initial concentration on sorption. The results showed that, as the concentration of lead and cadmium increased from (50 - 250 mg/L), the amount of lead and cadmium adsorbed increased from 4.8600 to 24.1796 mg/g and 4.063 to 16.126 mg/g, respectively, implying the availability of adsorbate in the adsorption process [13]. This is connected with the competitive diffusion process of the lead and cadmium through the adsorbent [16]. This implies that an increase in concentration causes the adsorbate ions to compete strongly for the adsorption site capacity [17].

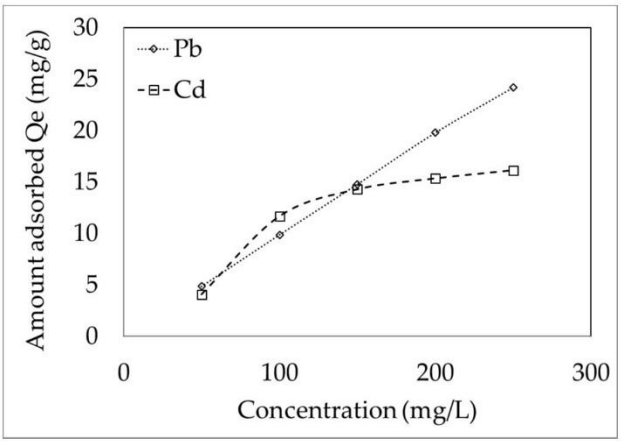

Figure 4. Effect of concentration on adsorption of Pb^{2+} and Cd^{2+} by VSS.

3.3. Adsorption kinetic modeling

The results from the kinetic parameters in Table 2 and Fig. 5 showed that the adsorption of lead and cadmium ions could be described by both first and second order models [13]. Based on the correlation coefficient R^2, it was observed that the Blanchard pseudo-second order best described the entire adsorption process with higher R^2 values of (0.9999) for lead and (0.9998) for cadmium respectively. The pseudo-second order rate constants K_2 were found to be (0.379 $g.mg^{-1}min^{-1}$) and (-0.0609 $g.mg^{-1}min^{-1}$) for lead and cadmium respectively. This further implies that the adsorption of lead and cadmium onto VSS

Table 2. Kinetic parameter of Lagergren first order and blanchard second order for adsorption of lead and cadmium onto VSS adsorbent.

Adsorbent	Model	Adsorbate	Adsorbate
	First order	*Lead*	*Cadmium*
VSS	K_1 ($Lmin^{-1}$)	0.0156	0.00345
	Qe (mg/g)	0.194	0.148
	R^2	0.0800	0.0086
	Second order	*Lead*	*Cadmium*
VSS	K_2 ($g.mg^{-1}min^{-1}$)	0.379	-0.0609
	Qe (mg/g)	5.0075	4.051
	R^2	0.9999	0.9998
	h ($gmg^{-1}min^{-1}$)	9.503	0.999

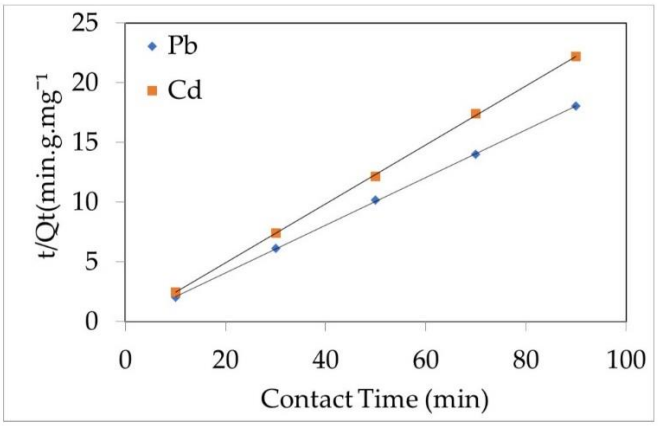

Figure 5. Blanchard pseudo-second order kinetic plots for Pb and Cd on VSS adsorbent.

adsorbent may have occurred through a weak physical interaction caused by Vander Waals forces [17]. A summary of the kinetic parameters of pseudo first and second order for adsorption lead and cadmium onto the VSS adsorbent is presented in Table 2.

3.4. Adsorption isotherm models

The results obtained from the Langmuir and Freundlich adsorption isotherm models for; Pb^{2+} and Cd^{2+} ions are presented in Table 3. For the Langmuir model, the maximum adsorption capacity, Q_m for lead and cadmium were found to be (434.78) mg/g and (4.293) mg/g for VSS, respectively, which represents, the total adsorbate–adsorbent binding capacity [17]. The separation factor (R_L) which describes the suitability of the VSS adsorbent and its affinity towards Pb (II) and Cd (II) ions was determined. Four probabilities exist for the value of R_L: $R_L > 1$, $R_L = 1$, $0 < R_L < 1$, and $R_L = 0$, indicating unfavorable, linear,

https://doi.org/10.58985/jesec.2025.v01i02.09

Table 3. Isotherm parameters for lead and cadmium adsorption on adsorbents.

Adsorbent	Model	Adsorbate	Adsorbate	Model	Adsorbate	Adsorbate
	Langmuir	*Lead*	*Cadmium*	*Freundlich*	*Lead*	*Cadmium*
VSS	Q_m(mg/g)	434.78	4.293	1/n	0.621	3.052
	b (L/mg)	0.013	0.053	n_F	1.608	0.327
	R^2	0.469	0.962	R^2	0.532	0.987
	R_L	0.606	0.273	K_F mg/g(mg/L)^n	7.612	0.005

Table 4. Thermodynamic parameters of adsorption for lead and cadmium.

Adsorbates	Adsorbent	ΔH (kJ/mol.)/1000	ΔS (J/molK)	R^2	ΔG (kJ/mol.)/1000
Lead	VSS	6.265	27.158	0.0085	-2.507
Cadmium	VSS	1.348	-4.426	0.1469	2.910

suitable, and irreversible degrees, respectively. From the results obtained, the calculated Langmuir separation factor R_L, for Pb (II) and Cd (II) metal ions were found to be 0.606 and 0.273 respectively, indicating the suitability of the adsorption process [16]. The results of correlation coefficients R^2 of the Freundlich gave higher R^2 values than Langmuir isotherm, indicating that the experimental data best obeyed the Freundlich isotherm for both lead and cadmium. This implies that the uptake of lead and cadmium analytes occurred on a heterogeneous surface by multilayer adsorption and there is a non-uniform distribution of the heat of adsorption over the VSH surface [16]. The Freundlich results showed that the value of $\frac{1}{nF}$ is less than unity for lead and greater than unity for cadmium indicating favourable and unfavourable adsorption onto VSS respectively [13]. For the nF values, if nF = 1, the adsorption is linear; if nF < 1, the adsorption process is chemical, and if nF > 1, the adsorption is a favourable physical process [14]. From the result, the nF values for lead and cadmium were found to be 1.608 and 0.327, respectively indicating favourable physical and chemical adsorption process [13].

3.5. Thermodynamics parameter for adsorption of lead and cadmium

The calculated values of the thermodynamic parameters for the Gibbs free energy change (ΔG), enthalpy change (ΔH) and entropy (ΔS) in this study are presented in Table 4. The calculated ΔH^0 are positive values found to be 6.265 kJmol^{-1} and 1.348 kJmol^{-1} for lead and cadmium, respectively. A positive ΔH^0 indicates an endothermic reaction, hence, physisorption dominates chemisorption [16]. Therefore, high temperature does not favor the adsorption of lead and cadmium. From Table 4, the ΔS^0 for lead and cadmium was found to be 27.158 and - 4.426 J/molK, respectively. The positive value of (27.158 J/molK) for ΔS^0 for lead indicates of spontaneous process [13]. While the negative value of ΔS^0 for Cadmium reveals a non-spontaneous adsorption [14].

4. Conclusions

The adsorption of lead and cadmium is affected by the initial pH, adsorbent dosage, initial solution concentrations, temperature and contact time. From the investigation, the adsorption capacity of lead and cadmium decreased with an increase in the adsorbent dosage for VSS. A pH 12 was found to be the optimum pH for adsorption of lead and cadmium respectively. For the effects of initial solution concentration and temperature, it was found that adsorption capacity of VSS increased with increasing in concentration and temperature for lead and cadmium. The adsorption isotherm and kinetics of the process favored the Freundlich isotherm and pseudo-second order models suggesting a multilayer adsorption. The results, indicated that physisorption dominated chemisorption. The *Vigna subterranea* shells (VSS) adsorbent displayed remarkable efficiency and effectiveness in the removal of lead and cadmium and can be recommended for the removal of other environmental pollutants.

https://doi.org/10.58985/jesec.2025.v01i02.09

Disclaimer (artificial intelligence)

Author(s) hereby state that no generative AI tools such as Large Language Models (ChatGPT, Copilot, etc.) and text-to-image generators were utilized in the preparation or editing of this manuscript.

Authors' contributions

Project conceptualization, design, and supervision, G.O.E.; writing, results extraction, analysis, and manuscript first draft, F.T.S.; manuscript revision, review, and proofreading, E.A.Y., A.R.O.A.; resources, review, and editing, S.A.N.

Acknowledgements

The authors acknowledge the support of the Chemical Society of Nigeria (CSN) released for the 46th Annual International Conference, Workshop & Exhibition, Awka 2023.

Funding

This research was not funded by any Governmental or Non-governmental agency.

Availability of data and materials

The data used to support the findings of this study can be obtained from the corresponding author upon request.

Conflicts of interest

All authors declare zero conflict of interest that could have influenced the research work.

References

1. Chiban, M.; Soudani, A.; Sinan, F.; Persin, M. Wastewater treatment by batch adsorption method onto microparticles of dried *Withania frutescens* plant as a new adsorbent. J. Environ. Mgt. 2012, 95, 61–65. https://doi.org/10.1016/j.jenvman.2011.06.044
2. Badmus, M.A.O.; Audu, T.O.K.; Anyata, B.U. Removal of lead ion from industrial wastewaters by activated carbon prepared from periwinkle shells. Turkish J. Engin. Environ. Sci. 2007, 31, 251–63. https://doi.org/10.1007/s11814-007-5049-5
3. Otitoju, O.; Ezeonu, C.S. Quantification of nitrate, chlorophyll and zinc in *Manihot esculentum* leaves from farmland along Uyo municipal waste dump. J. Res. Environ. Sci. Toxic. 2014, 3(3), 30-33. http:/dx.doi.org/10.14303/jrest.2014.011
4. Denkhaus, E.; Salnikov, K. Nickel essentiality, toxicity and car-cinogenicity, Critical Review. J. Hemato Oncol. 2002, 42, 35–56. https://doi.org/10.1016/s1040-8428(01)00214-1
5. Dawodu, F.A.; Akpomie, G.K.; Ogbu, I.C. Application of kinetic rate equations on the removal of copper (II) ions by adsorption unto aloji kaolinite clay mineral. Intl. J. Multidisc. Sci. Engin. 2012, 3(10), 1-6. https://doi.org/10.1016/j.jmrt.2014.03.002
6. Wang, S.; Li, H. Kinetic modeling and mechanism of dye adsorption on unburned carbon. J. Dyes Pigment. 2007, 72, 308–314. https://doi.org/10.1016/j.dyepig.2005.09.005
7. Adelagun, R.O.A.; Berezi E.P.; Itodo, A.U.; Oko, O.J.; Kamba, E.A.; Andrew, C.; Bello, H.A. Adsorption of Pb^{2+} from aqueous solution by modified melon (*Citrullus lanatus)* seed husk. J. Chem. Mater. Res. 2014, 6 (2), 113-121. www.iiste.org/Journals/index.php/CMR/article/view/10863
8. Mamdoutth, N.N.; Kamar, T.E.; Ebrahiem, H.M.; Manssour, H.M. Adsorption of iron and manganese ions using low cost materials as adsorbent. Adsorpt. Sci. Tech. 2024, 22(1), 25-37. https://doi.org/10.1260/026361704323150971
9. Mohammad, W.A.; Fawwaz I.K.; Akl A.M. Adsorption of lead, zinc and cadmium ions on polyphosphate-modified kaolinite clay. J. Environ. Chem. Ecotox. 2010, 2(1), 001-008.
10. Baryeh, E.A. Physical properties of bambara groundnuts. J. Food Eng. 2001, 47, 321-326. https://doi.org/10.1016/s0260-8774(00)00136-9
11. Johari, K.; Saman, N.; Song, S.T.; Heng, J.Y.Y.; Mat, H. Study of Hg (II) removal from aqueous solution using Lignocellulosic coconut fiber biosorbents: Equilib. Kinet. Eval. 2014, 1198-1220. https://doi.org/10.1080/00986445.2013.806311
12. Okeke, E.C.; Eze, C. Nutrient composition and nutritive cost of Igbo traditional vendor foods and recipes commonly eaten in Nsukka. J. Agric. Food, Environ. Ext. 2006, 5(1), 36-44. https://doi.org/10.4314/as.v5i1.1542
13. Egah, G.O.; Baba, N.H.; Ngantem, G.S.; Yerima, E.A.; Omovo M. Synergistic study of hydroxyiron (iii) and kaolinite composite for the adsorptive removal of phenol and cadmium. Int. J. Environ. Chem. 2019, 3(1), 30-42. https://doi.org/10.11648/j.ijec.20190301.15
14. Sha'Ato, R.; Egah, G.O.; Itodo A.U. Aqueous phase abatement of phenol and cadmium using Hydroxyiron (III) calcined with bentonite. J. Fuw Trends Sci. Technol. 2018, 3 (1), 1-10.
15. Adelagun, R.O.A.; Itodo, A.U.; Berezi, E.P.; Oko, O.J.; Kamba, E.A.; Andrew, C.; Bello, H.A. Adsorptive

removal of Cd^{2+} and Zn^{2+} from aqueous system by BSG. J. Chem. Mater. Res. 2014, 6 (2), 104-112. https://www.iiste.org/Journals/index.php/CMR/article/viewFile/10862/11165

16. Sodeinde, K.O.; Olusanya, S.O.; Momodu, D.U.; Enogheghase, V.F.; Lawal, O.S. Waste glass: An excellent adsorbent for crystal violet dye, Pb^{2+} and Cd^{2+} heavy metal ions decontamination from wastewater, J. Niger. Soc. Phys. Sci. 2021, 3, 414–422. https://doi.org/10.46481/jnsps.2021.261
17. Tatah, V.S.; Otitoju, O.; Ezeonu, C.S.; Onwurah, I.N.E.; Ibrahim, K.L.C. Characterization and adsorption isotherm studies of Cd (II) and Pb (II) ions bioremediation from aqueous solution using unmodified sorghum husk. Appl. J. Biotechno. Bioengin. 2017, 2(3), 113 - 120. https://doi.org/10.15406/jabb.2017.02.00034
18. Jameel, M.D.; Hussien, A.K.; Nasser, T. Removal of cadmium ions from industrial waste water using Iraqi ceatophyllum Demersum. AL- Mustansiriyah. J. Sci. 2012, 32 (8), 71-84.
19. EL-Dars, E.S.M.F.; Ibrahim, M.H.; Farag, B.A.H.; Abdelwahhab, Z.M.; Shalabi, H.E.M. Preparation and characterization of bentonite carbon composite and design application in adsorption of bromothymol blue dye. J. Multidis. Eng. Sci. Tech. 2016, 3(1), 3758-3765.
20. Kibami, D.; Pongener, C.; Rao, K.S.; Sinha, D. Preparation and characterization of activated carbon from *Fagopyrum esculentum* Moench by HNO_3 and H_3PO_4 chemical activation. Der. Chem. Sinica. 2014, 5(4), 46-55.

https://doi.org/10.58985/jesec.2025.v01i02.09